Combining VTI and HTI anisotropy in prestack time migration: Workflow and data examples

Edward Jenner, ION

Accounting for anisotropy in P-wave data processing is now recognized as an important step in improving the quality of seismic data. The quality of final migrated images, prestack gathers, and any attributes derived from the seismic data can all be improved. Commonly, two forms of anisotropy are considered. The first and most common is vertical transverse isotropy (VTI), or the closely associated tilted transverse isotropy (TTI). This anisotropy is often caused by fine layering of sediments, with the layering smaller in scale than the seismic wavelength. In the case of VTI the bedding planes are horizontal, while in TTI they are dipping.

Both these forms of anisotropy cause the well-known "hockey stick" or nonhyperbolic moveout effect on NMO-corrected gathers at long offsets (typically beyond offset-to-depth ratios of 1.0). In addition, TTI anisotropy causes an azimuthal variation of traveltimes; however, this type of anisotropy is mostly considered in depth processing. In the TTI case, the anisotropy parameters are partially controlled by well data and the symmetry plane is normally assumed to be parallel to the bedding. For time processing, it is more usual to account for VTI anisotropy; azimuthal traveltime variations are not considered and the anisotropic parameters required for time imaging can be obtained from the seismic data alone.

The second form of anisotropy considered in P-wave processing is horizontal transverse isotropy (HTI). The most commonly considered mechanism for this type of anisotropy is vertical aligned fractures embedded in an isotropic background medium. This type of anisotropy causes azimuthal traveltime variations which can become apparent at near-to-mid offsets (offset-to-depth ratios of 0.5 and beyond).

In reality, the subsurface is likely to contain both types of anisotropy, either combined or in separate layers. For a medium with vertical aligned fractures embedded in a finely layered background, the result is a medium that exhibits orthorhombic symmetry. In the general case, this requires the estimation of many more parameters than that of VTI and HTI media separately and parameter estimates can easily become unstable when inverting typical field data. In this paper, I propose an approximate but stable method to correct data for the effects of a combination of VTI and HTI anisotropy in prestack time migration (PSTM). The effectiveness of the method is demonstrated with field data examples.

Theory and practical considerations

P-wave reflection moveout in an orthorhombic layer consisting of vertical aligned fractures embedded in a finely layered and horizontally stratified medium can be approximated by the equation:

$$T^2(x,\alpha) = T_0^2 + \frac{x^2}{V_{nmo}^2(\alpha)} - \frac{2\eta(\alpha)x^4}{V_{nmo}^2(\alpha)\left\{T_0^2 V_{nmo}^2(\alpha) + [1 + 2\eta(\alpha)]x^2\right\}} \quad (1)$$

T is the total traveltime, T_0 is the zero-offset traveltime, x is the source-receiver offset, $V_{nmo}(\alpha)$ is the azimuthally varying NMO velocity, $\eta(\alpha)$ is the azimuthally varying Alkhalifah-Tsvankin parameter (Alkhalifah and Tsvankin, 1995) for VTI anisotropy, and α is the difference between the source-receiver line and the fracture direction.

$V_{nmo}(\alpha)$ is given by (Grechka et al., 1999):

$$\frac{1}{V_{nmo}^2(\alpha)} = \frac{\cos^2(\alpha)}{V_{fast}^2} + \frac{\sin^2(\alpha)}{V_{slow}^2} \quad (2)$$

V_{fast} and V_{slow} are, respectively, the NMO velocities parallel and perpendicular to the fracture direction. $\eta(\alpha)$ is given by (Pech and Tsvankin, 2004)

$$\eta(\alpha) = \eta^{(1)}\sin^2(\alpha) - \eta^{(3)}\sin^2(\alpha)\cos^2(\alpha) + \eta^{(2)}\cos^2(\alpha) \quad (3)$$

where $\eta^{(1,2,3)}$ are parameters controlling the azimuthal variation of η.

In this paper, I shall often refer to the offset-to-depth ratio as ODR, the ratio of the offset of a trace at a particular reflection event to the depth of the zero-offset traveltime of that event. Clearly, for time processing with no well control, this is an approximation, but is important when considering which terms of Equation 1 may dominate for a particular offset and time.

An approximate traveltime equation for a purely VTI medium can be obtained by replacing $V_{nmo}(\alpha)$ and $\eta(\alpha)$ with their non-azimuthally varying counterparts V_{nmo} and η. For an HTI medium, the near-offset variation in NMO velocity is obtained by setting $\eta(\alpha) = 0$ and thus eliminating the third term in Equation 1.

At this stage, we have at least six unknowns: V_{fast}, V_{slow}, $\eta^{(1)}$, $\eta^{(2)}$, $\eta^{(3)}$ and α. T_0 may be treated as known or unknown depending on the inversion scheme, but in any case T_0 is usually well resolved. However, Equation 1 is valid only for a single layer or multiple layers where the fracture orientation does not vary with depth. In practice, we observe that the fracture orientation may vary substantially with depth, and in this case, the azimuth η in Equation 3 is not the same as the azimuth α in Equation 2. This results in an additional azimuth to be estimated. Thus, the azimuthal variation of η can be of a different magnitude and orientation than the variation in NMO velocity and is not elliptical (although it may be close to an ellipse for small $\eta^{(1)}$ and $\eta^{(2)}$, and if $\eta^{(3)} \approx 0$).

In the case of pure HTI media, three parameters need to be inverted (V_{fast}, V_{slow}, and α) and this is often a stable

inversion for wide-azimuth acquisition geometries where the data contain sufficient offsets and azimuths at the target horizon. In addition, because data at offsets less than ODRs of 1.0–1.2 are inverted, they are less susceptible to lateral velocity heterogeneities and are often less noisy than far-offset data. Furthermore, even quite large lateral velocity variations will produce traveltime variations that conform to Equation 2 (Jenner, 2010). Thus, although the true anisotropy may be distorted and subsequent interpretation hampered by lateral heterogeneity, the traveltime inversion can still fit the data to Equation 2.

On the other hand, determination of VTI anisotropy requires just two parameters (V_{nmo} and η). Despite this, obtaining reliable estimates of η for land seismic data can be difficult. The inversion relies on the farthest offsets; however, offsets in field data are often restricted to ODRs of significantly less than 2.0, and the far offsets may be contaminated with coherent noise such as converted-wave energy. In addition, unlike HTI anisotropy, traveltimes in a VTI medium that are distorted by lateral velocity variations do not conform to Equation 3 (Takanashi and Tsvankin, 2010). Coupled with the fact that lateral velocity variations are more likely to be encountered because of the larger spread length, it is perhaps not surprising that the inverted η values tend to be less laterally coherent than V_{fast} and V_{slow} inverted from the near to mid offsets. Thus, they often require more smoothing to obtain stable results.

Finally, it is also well known that there is an inherent trade-off between determining η and V_{nmo}, particularly when data do not have sufficiently large offsets. Thus, the possibility of lateral heterogeneity and noise encountered in the long spread lengths required for reliable η estimation will impact the inverted V_{nmo}. Therefore, inverting Equation 1 directly requires high-quality data with long offsets (ODRs of 2.0 or greater) in a wide range of azimuths. If one were to attempt a straight inversion of Equation 1, instabilities in the estimates of $\eta^{(1)}$, $\eta^{(2)}$, and $\eta^{(3}$ would adversely affect V_{fast} and V_{slow}.

One final point that I would like to consider in this section is that of smoothing. Noise in inversion results means that we need to perform some type of smoothing both spatially and temporally. This may simply be applying a smoothing algorithm to the output inversion parameters, or having some more global inversion with constraints to ensure the output parameters have a certain smoothness. The former is more commonly used and is certainly effective when dealing with isotropic velocities or V_{nmo} and η from a VTI inversion. However, for a near-offset HTI inversion (or for inverting Equation 1), one cannot simply smooth the parameters V_{fast}, V_{slow} and α. For instance, consider the case where we have two NMO ellipses with the same V_{fast} and V_{slow} but azimuths differing by 90°. Averaging the traveltimes should give an isotropic response, but averaging V_{fast} and V_{slow} separately will maintain the anisotropy. This would also occur if one were to average a larger number of ellipses with radom orientations, which is perhaps more intuitively isotropic.

For the HTI equation, where we ignore the far-offset traveltime variation, there is an elegant solution to this issue.
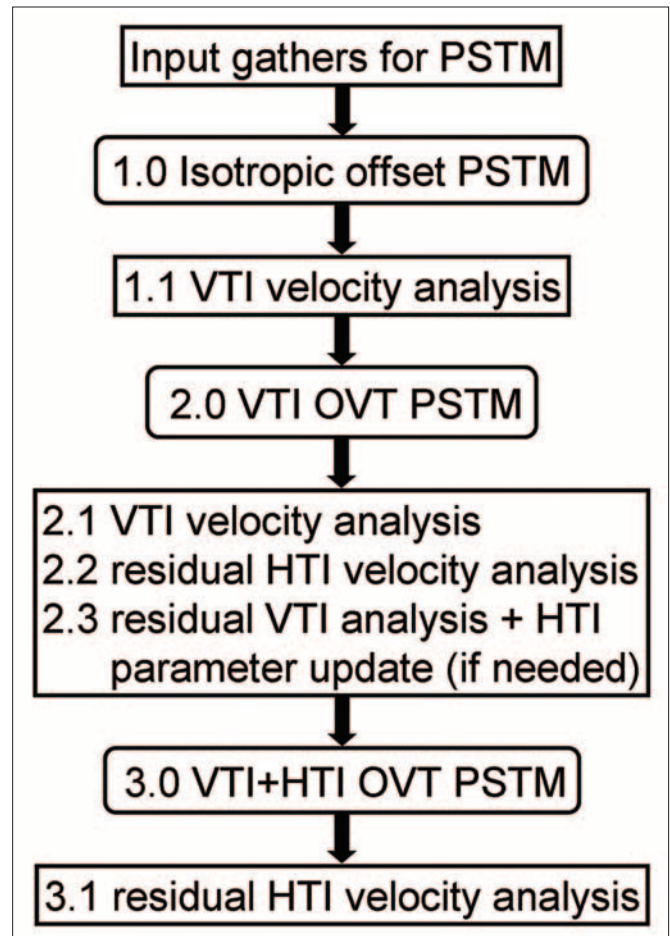

Figure 1. *Summary of the VTI+HTI workflow used for combined VTI and HTI parameter estimation and prestack time migration.*

Equation 2 can be rewritten as a linear combination of three parameters (I refer to them here as "ellipse coefficients") that are related through trigonometric expressions to V_{fast}, V_{slow}, and α (Grechka et al., 1999). A linear inversion of the traveltimes is performed to obtain these ellipse coefficients which can then be individually filtered as long as the same filter is applied to each of the coefficients. Normalizing the filter is required to maintain the values of V_{fast} and V_{slow}.

However, for Equation 1 no such linearization is possible. In addition, as discussed earlier, we would like to be able to smooth some parameters such as η more than other parameters such as the ellipse coefficients (related to V_{fast}, and V_{slow}).

Method

In practice, land seismic data may be acquired with a good azimuth distribution for near to mid offsets and perhaps have some longer offsets in a narrow azimuth range (as in a rectangular patch). The wide-azimuth data allow us to determine the near-to-mid offset azimuthal variation in NMO velocity. However, the long-offset data are usually insufficient to accurately estimate an azimuthally varying η, particularly one that may have a complex traveltime surface. Therefore, I propose a method that separately inverts for HTI and VTI
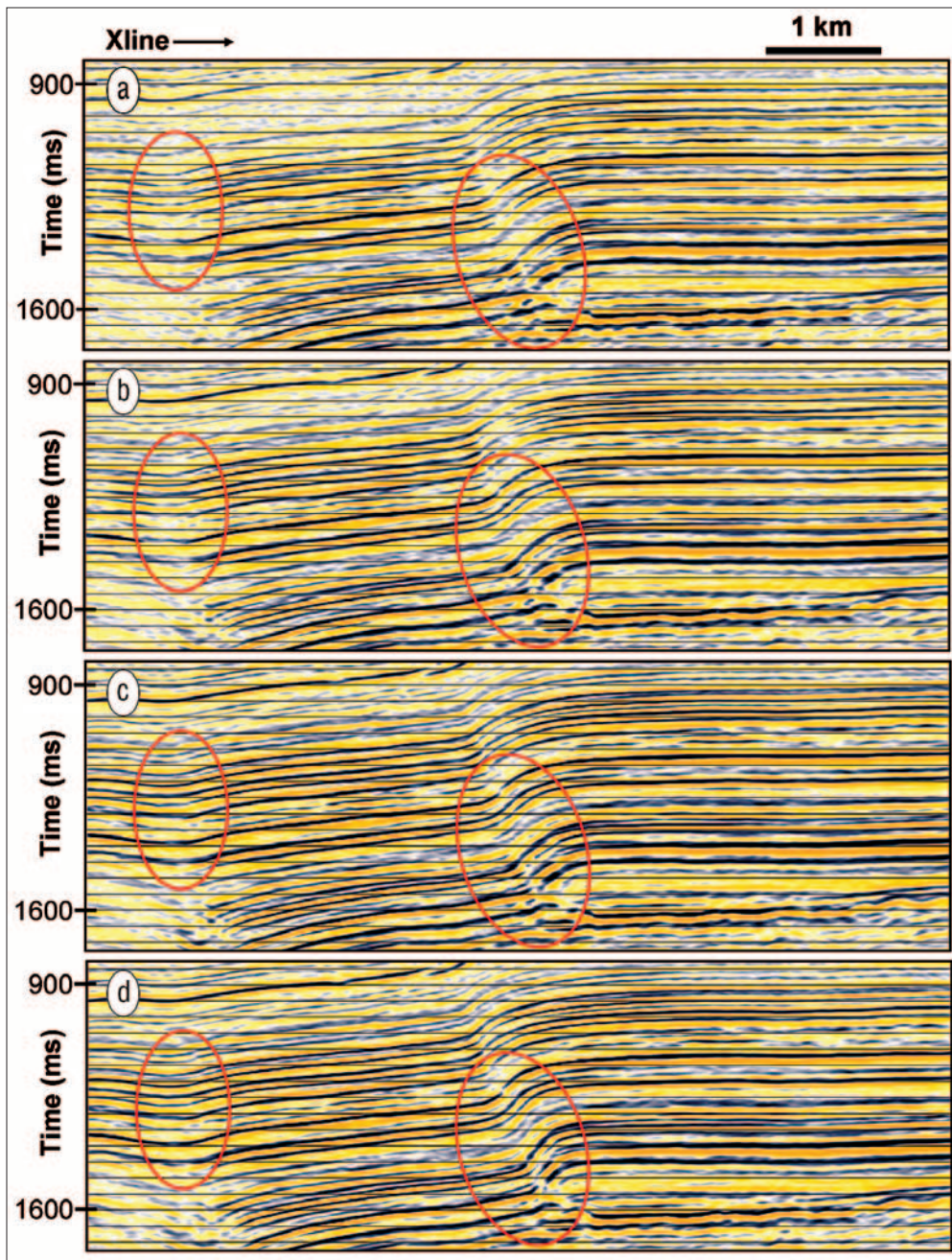
Figure 2. OVT migrations through an inline using various velocity fields: (a) isotropic velocity field; (b) VTI velocity field, (c) VTI velocity field with residual VTI and HTI corrections; and (d) combined VTI+HTI velocity field followed by residual HTI correction. Red ellipses indicate areas of the most significant improvements.

parameters but couples them so that the near-offset traveltimes are consistent. An outline of the "VTI + HTI" flow is given in Figure 1. Standard processing is used as the input to prestack time migration (PSTM) with the caveat that any multitrace filtering should preserve azimuthal traveltime and amplitude information. A conventional offset PSTM is used with a first pass of isotropic velocities to migrate the data. V_{nmo} and η are then simultaneously inverted for the long-offset nonhyperbolic NMO. This could be a manual picking program or more likely an automated semblance-picking algorithm with user QC and adjustments. In any case, it is important to simultaneously scan both V_{nmo} and η since the initial isotropic velocity, or subsequent V_{nmo} estimates using just the near-mid offsets are likely to be distorted when VTI

anisotropy is present. For instance, if the CMP gathers are aligned to an ODR of 1.0 using a hyperbolic NMO velocity, then that velocity will need to be reduced when applying a positive η correction to flatten the far offsets while simultaneously maintaining the alignment at near offsets.

The analysis of V_{nmo} and η on CMP gathers is only reliable, however, where the data have sufficient offsets and thus a sufficient maximum ODR. Thus, below a certain time, where the maximum ODR becomes too small, the analysis becomes unstable. If necessary, and particularly if there is significant structure, a VTI model at these later times can be built based on migration scans of combinations of V_{nmo} and η for target lines. For these scans, as η is adjusted, V_{nmo} is also adjusted so that the near-to-mid traveltimes obtained from isotropic

velocity analysis are maintained.

The obtained V_{nmo} and η are smoothed and then used as the input velocity field into an offset vector tile (OVT) PSTM (Vermeer, 2002; Calvert et al., 2008). This is a method of binning the data in a prestack migration that preserves both offset and azimuth information in an optimal way for surveys with a regular geometry. While most land seismic surveys are far from perfectly regular (skidded shots, areas of missing data, etc.), the technique is robust and can handle a significant departure from ideal acquisition geometries.

V_{nmo} and η are then repicked on a dense grid (usually every third inline and third crossline) using a simultaneous automatic traveltime inversion similar to the method proposed by Jenner (2001) for azimuthal velocity inversion. At this stage, the data are still contaminated with azimuthal NMO and thus may not give a well-defined semblance peak value for the appropriate V_{nmo} and η. The automatic traveltime inversion circumvents this issue by picking traveltimes and inverting those traveltimes for V_{nmo} and η, rather than using a semblance-based approach. The resulting inversion picks an average traveltime through the azimuthal variations. Thus, although the solution may have a high variance in areas of high azimuthal NMO, it is stable as long as reasonably accurate traveltimes can be picked.

After smoothing of V_{nmo} and η, the VTI correction is applied to the PSTM gathers and a second high-density automatic traveltime inversion is performed for the residual azimuthal variation of NMO velocity for ODRs less than ~1.0–1.3 (Equation 1 with η(α) = 0). The velocity inversion is performed as a residual around the VTI traveltimes. The inversion is also limited to the portion of the data that displayed approximately hyperbolic moveout prior to the VTI correction. This is because the azimuthal variation of apparent velocity at farther offsets is not necessarily elliptical and may be of a different magnitude and direction than the variation at near to mid offsets. In addition, those variations will be more sensitive to lateral heterogeneity. Therefore, attempting to invert for azimuthal NMO for long offsets may result in not properly characterizing the traveltime variations at near-to-mid offsets and instability in the inversion results. In addition, the results may be systematically biased by the offset range used in the inversion, causing temporal and spatial variations in anisotropy to be related to temporal and spatial variations in the maximum ODR used.

The azimuthal NMO inversion may result in V_{fast} and V_{slow} values whose average is different than the V_{nmo} picked in the VTI inversion. It is likely that these picks will more accurately align events than the VTI analysis because of the limited offset range used in the inversion, increased stability and less smoothing. However, there is also a possibility that a further update of η will be required. This can be achieved by running a second VTI inversion. This time after smoothing the η values, V_{fast}, and V_{slow} are recomputed by minimizing the difference between the traveltimes at near offsets between the previous (smooth) η and the updated (smooth) η. This ensures that the near-offset data remain aligned while the updated η flattens the far offsets. This method allows a much
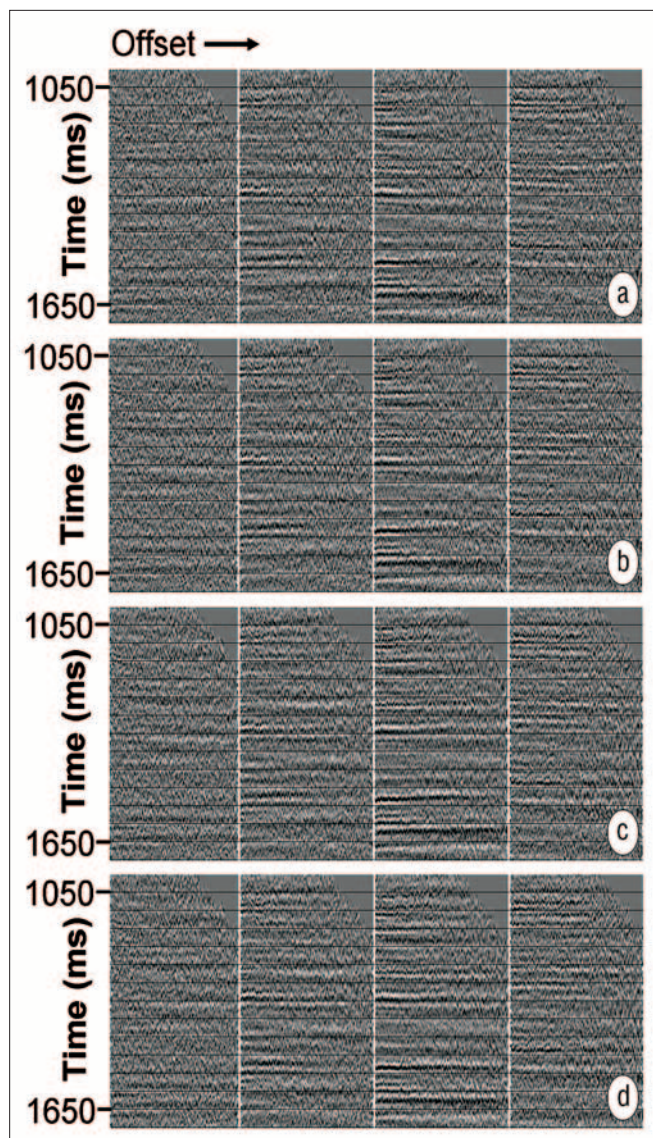

Figure 3. *Four OVT CMP gathers migrated with various velocity fields and sorted as a function of offset: (a) isotropic velocity field; (b) VTI velocity field; (c) VTI velocity field with residual VTI and HTI corrections; and (d) combined VTI+HTI velocity field followed by residual HTI correction.*

higher smoothing to be applied to η than to the azimuthal NMO ellipse coefficients and allows control between the accuracy in aligning the near offsets and any lack of stability due to noise and lateral heterogeneity.

The four parameters (V_{fast}, V_{slow}, azimuth of V_{fast} and η) are then used to compute traveltimes for a second pass of OVT PSTM. Because the NMO ellipse coefficients and thus V_{fast}, V_{slow} and the azimuth of V_{fast} are smoothed for migration, a second pass of residual azimuthal NMO inversion is performed prior to stacking the migrated OVT data. One could also perform a residual η analysis at this stage, with the appropriate change in V_{fast} and V_{slow} to maintain near-offset alignment. This may be particularly beneficial if AVO or if inversions are to be performed on the output gathers.
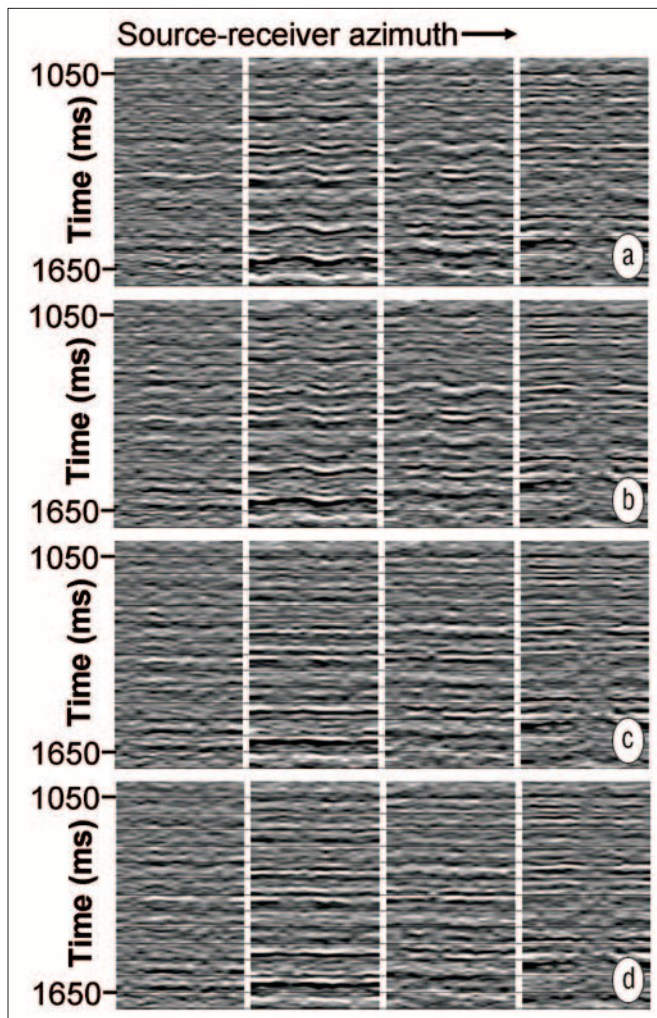
Figure 4. *Four OVT CMP gathers migrated with various velocity fields and sorted as a function of source-receiver azimuth: (a) isotropic velocity field; (b) VTI velocity field; (c) VTI velocity field with residual VTI and HTI corrections; and (d) combined VTI + HTI velocity field followed by residual HTI correction.*

Field data example

The Durham Ranch seismic survey comprises 80 km^2 in the Sand Wash Basin in northern Colorado. It was shot with source lines orthogonal to the receiver lines and source and receiver line intervals of 151 m and source and receiver station intervals of 50 m. The source was a mix of vibroseis and dynamite. The main target in this area is the Niobrara Formation at 350–900 m depth. For the purpose of demonstrating the workflow, however, I will concentrate on the deeper, more structural formations where there is a more obvious requirement for PSTM to properly image the reflections. A more detailed discussion of the area, the seismic survey, and processing has been provided by Schapper et al. (2009).

An overview of the VTI + HTI workflow is given in Figure 1 and I shall refer to the workflow "steps" by the numbers given in that figure. In order to facilitate direct comparison of gathers and stacks, all data were migrated with the same parameters and stacked with the same mute. This means that instead of an offset PSTM in step 1.0, I performed an OVT PSTM. While similar results are obtained, an offset PSTM
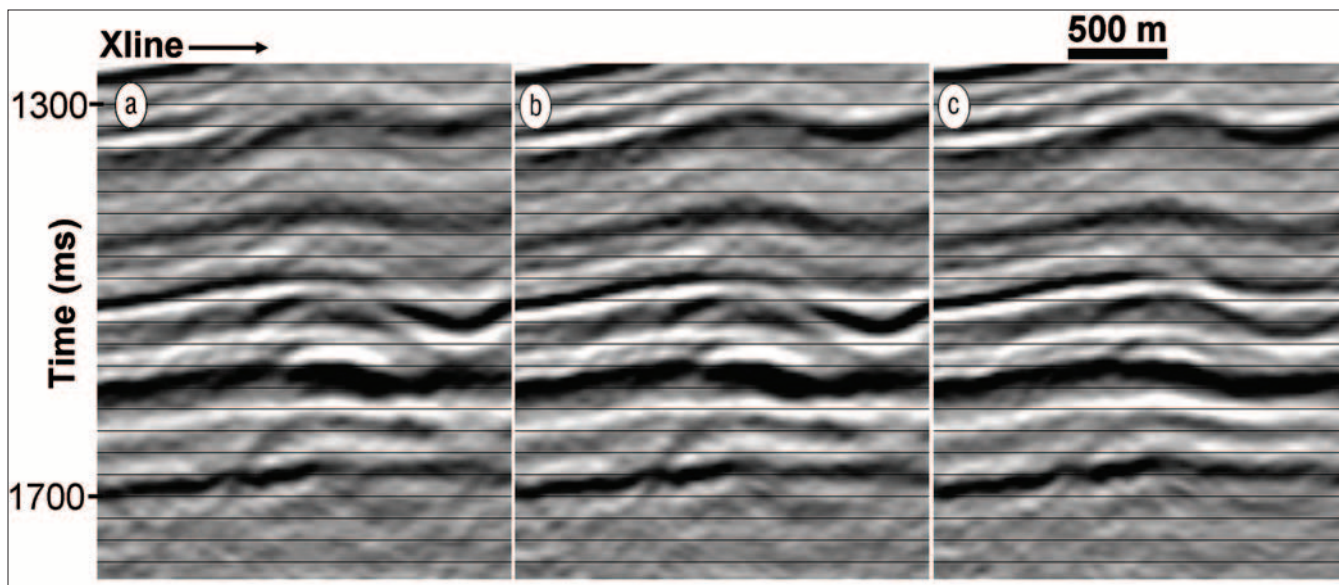
Figure 5. Portion of OVT prestack time migrations migrated with (a) VTI velocity field, (b) VTI velocity field with residual VTI and HTI corrections, and (c) combined VTI+HTI velocity field followed by residual HTI correction.

makes picking the VTI parameters easier at this stage. The maximum dip used in all migrations was 60° with the maximum structural dip being approximately 40–50°. Increasing the maximum dip in the migration did not appear to improve the steep-dip imaging. Using the same mute is clearly not optimal for each individual migration and the mute used was very open (ODR = 1.5, or ~40–45° incidence angle). In particular, one would expect that a VTI migration would allow farther offsets to be stacked coherently than an isotropic migration. So, while this may not be the optimal imaging mute for any of the individual migrations, it serves to demonstrate the potential differences at each step of the workflow.

The farthest offset with a good azimuth distribution in the data was 2600 m and the approximate depth to the reflectors displayed in Figures 2–4 is 1500–3300 m. The shallower reflections are within the mute zone and have maximum useful ODRs of ~1.7, while the deeper reflections have ODR of less than 1.0. Thus a wide range of ODRs is spanned which is often the case in field data and which any workflow must deal with successfully. For the data with ODRs greater than approximately 1.4, the VTI inversion on CMP gathers allowed for estimating V_{nmo} and η after removing outliers and appropriate smoothing. Below this, η was estimated by migration scans while changing V_{nmo} to maintain the near-offset traveltimes. Although the offset range is not large enough for stable inversions, the reflection events sometimes display some curvature between the near and mid offsets. The gathers were therefore inspected to ensure they remain flat and excess curvature at the near-mid offsets had not been introduced after the VTI migration.

Figures 2–4 show stacks of the OVT migrations, offset-sorted gathers, and azimuth-sorted gathers, respectively, through the workflow outlined in Figure 1. Because the velocities are smoothed for the migration, I compare the VTI migration with the residual VTI + HTI correction to the VTI

+ HTI migration with the residual HTI correction. The applied velocity fields in both cases then have the same degree of smoothing applied.

Figure 2 compares the stacks through the workflow. The highlighted areas show where the most obvious improvements occur, although more subtle details are also significantly enhanced. The most substantial improvement occurs between Figures 2b and 2c, where the high-density VTI + HTI automatic traveltime inversion was performed. Although the first pass of η analysis was important in preparing the data for the high-density traveltime inversion, it does not appear to ubiquitously improve the stack and gathers. This is likely due to the fact that the inversion is noisy because the data are still contaminated with azimuthal NMO which is not handled well by semblance picking. Thus, a high degree of outlier removal and smoothing was applied to the resulting η field in step 1.1.

Figure 3 shows a representative sample of four CMP gathers, with varying degrees of noise, long-offset residual NMO and azimuthal NMO. The mute, which can be seen in the upper right portion of the gathers, is at an ODR = 1.5 and the maximum offset is 2600 m. The initial η analysis (Figures 3a and 3b) shows that where the data are reasonably continuous at far offsets, the η correction has better aligned the gathers. Again, the most significant improvements occur at step 2 in the workflow where the high-density residual η correction is applied, and the azimuthal NMO is accounted for. In particular, in the third gather, far offsets which appear to be completely dominated by random noise are well aligned after the azimuthal NMO correction. The gathers are similar after the final OVT migration, but reflector alignment is further improved after the residual azimuthal NMO correction in step 3.1 (Figures 3c and 3d).

The same gathers (and times) shown in Figure 3 are also displayed in Figure 4, but in this case sorted by source-receiver

azimuth. For this display, the data were stacked into 20°-azimuth sectors to ensure an even distribution and spacing of azimuths across the plot. In addition, only ODRs of 0.5–1.5 were included in the stacks because this is where the largest variations in traveltimes occur. The azimuthal anisotropy causes traveltime variations with azimuth that can be observed in Figure 4 as sinusoidal variations as a function of source-receiver azimuth. This level of anisotropy was not uncommon in the survey and even higher amounts were observed in some locations. The differences between Figures 3a and 3b are slight, but overall the VTI migration appears to have helped define the azimuthal traveltime variation. In this domain and at these locations, the HTI + VTI migration and residual azimuthal NMO correction did not result in obvious improvements over simply applying an azimuthal NMO correction to the VTI migration (Figures 3c and 3d).

So far I have implied that applying the VTI + HTI correction to the VTI migrated OVT gathers (steps 2.1–2.3 in Figure 1) does not result in a significant improvement over applying them in the migration (step 3.0). On the one hand this is reassuring because it suggests consistency within the workflow. On the other hand one would expect that prestack migration with these traveltimes should result in improved imaging. Indeed, this is the case in certain areas of the survey. Figure 2 shows the improvement in the most steeply dipping parts of the structure. While applying the VTI + HTI correction does significantly improve the continuity of events, it only mildly impacts the overall structure. Migrating with the inverted traveltime curves, however, does improve the stack in some areas, particularly areas of higher dip. The central red ellipses in Figures 2c and 2d highlight one such area where the dips are noticeably larger and focusing is improved.

Figure 5 shows another such area, which is not characterized by high dips but rather by structural complexity and anisotropy, that results in inaccurate focusing of diffractions with a VTI migration. The VTI migration shown in Figure 5a is already an improvement over the isotropic migration. Applying steps 2.1–2.3 in the workflow, shown in Figure 5b, helps improve the continuity of the reflections, particularly in the upper part of Figure 5b. However, it cannot account for the still imperfect migration in the middle and lower potions of the data shown in Figure 5. Only when the VTI + HTI traveltimes are incorporated into a migration (Figure 5c) are the diffractions properly collapsed, reflections more continuous and the structure properly imaged.

Conclusions

I have described a workflow that can be used to incorporate both long-offset nonhyperbolic traveltimes (VTI anisotropy) and azimuthally varying traveltime variations (HTI anisotropy) into a prestack time migration. The workflow separates the VTI and HTI components so that instabilities in estimating VTI parameters do not impact HTI parameter estimation. Still, it is important that the parameters are inverted in a consistent manner and changes in the VTI parameters, including smoothing, are reflected by appropriately modifying the HTI parameters.

Application of this workflow to field data shows that the inversion produced aligned gathers and improved prestack time migrations in the presence of both nonhyperbolic moveout and azimuthal velocity variation. **TLE**

References
Alkhalifah, T. and I. Tsvankin, 1995, Velocity analysis for transversely isotropic media: Geophysics, **60**, no. 5, 1550–1566, doi:10.1190/1.1443888.

Calvert, A., E. Jenner, R. Jefferson, R. Bloor, N. Adams, and R. Ramkhelawan, 2008, Preserving azimuthal velocity information: experiences with cross-spread noise attenuation and offset vector tile PreSTM: 78th Annual International Meeting, SEG, Expanded Abstracts, 207–211.

Grechka, V., I. Tsvankin, and J. K. Cohen, 1999, Generalized Dix equation and analytic treatment of normal-moveout velocity for anisotropic media: Geophysical Prospecting, **47**, no. 2, 117–148, doi:10.1046/j.1365-2478.1999.00120.x.

Jenner, E., 2001, Azimuthal anisotropy of 3-D compressional wave seismic data, Weyburn Field, Saskatchewan, Canada: Ph.D. thesis, Colorado School of Mines.

Jenner, E., 2010, Modelling azimuthal NMO in laterally heterogeneous HTI media: First Break, **28**, 89–94.

Pech, A. and I. Tsvankin, 2004, Quartic moveout coefficient for a dipping azimuthally anisotropic layer: Geophysics, **69**, no. 3, 699–707, doi:10.1190/1.1759456.

Takanashi, M. and I. Tsvankin, 2010, Correction for the influence of velocity lenses on nonhyperbolic moveout inversion for VTI media: 80th Annual International Meeting, SEG, Expanded Abstracts, 238–243, doi:10.1190/1.3513330.

Schapper, S., R. Jefferson, A. Calvert, and M. Williams, 2009, Anisotropic velocities and offset vector tile prestack-migration processing of the Durham Ranch 3D, Northwest Colorado: The Leading Edge, **28**, no. 11, 1352–1361, doi:10.1190/1.3259614.

Vermeer, G. J. O., 2002, 3D seismic survey design: SEG.

Corresponding author: Edward.jenner@iongeo.com